


AXL signaling in primary sensory neurons contributes to chronic compression of dorsal root ganglion-induced neuropathic pain in rats

Molecular Pain
Volume 16: 1–13
© The Author(s) 2020
Article reuse guidelines:
sagepub.com/journals-permissions
DOI: 10.1177/1744806919900814
journals.sagepub.com/home/mpx


Lingli Liang^{1,2} , Jun Zhang³, Lixia Tian^{1,2}, Shuo Wang^{1,2},
Linping Xu^{1,2}, Yingxuan Wang¹, Qingying Guo-Shuai¹, Yue Dong¹,
Yu Chen¹, Hong Jia^{1,2}, Xuewei Yang³, and Chunmei Yuan³

Abstract

Low back pain is a chronic, highly prevalent, and hard-to-treat condition in the elderly. Clinical studies indicate that AXL, which belongs to the tyrosine kinase receptor subfamily, mediates pathological pain. However, it is not clear exactly how AXL regulates pain behaviors. In this study, we used a model of chronic compression of dorsal root ganglion-induced neuropathic pain to recreate clinical intervertebral foramen stenosis and related lumbocrustral pain to explore whether AXL in primary sensory neurons contributes to this neuropathic pain in rats. Using double-labeling immunofluorescence, we observed that both phosphorylated AXL and AXL were localized primarily on isolectin B4-positive and calcitonin gene-related peptide-positive neurons, while AXL was also localized in neurofilament-200-positive neurons. Chronic compression of dorsal root ganglion-induced pain was associated with the upregulation of AXL mRNA and protein in injured dorsal root ganglia. Repeated intrathecal administration of the AXL inhibitor, TP0903, or the AXL small interfering RNA effectively alleviated chronic compression of dorsal root ganglion-induced pain hypersensitivities. Moreover, repeated intrathecal administration of either TP0903 or AXL small interfering RNA reduced the expression of mammalian target of rapamycin in injured dorsal root ganglia, suggesting that mammalian target of rapamycin may mediate AXL's actions. These results indicate that the upregulation of dorsal root ganglion AXL may be part of a peripheral mechanism of neuropathic pain via an intracellular mammalian target of rapamycin-signaling pathway. Thus, while AXL inhibitors have so far primarily shown clinical efficacy in tumor treatment, AXL intervention could also serve as a potential target for the treatment of neuropathic pain.

Keywords

AXL, mammalian target of rapamycin, chronic compression of dorsal root ganglion, neuropathic pain, dorsal root ganglion

Date Received: 6 September 2019; revised: 25 November 2019; accepted: 17 December 2019

Introduction

Neurogenic chronic pain is a commonly occurring form of intractable pain in clinical practice, for which current analgesic drug treatments are relatively ineffective, with negative effects on patients' quality of life. At present, an urgent need exists for the development of novel, more effective drug treatments for neuropathic pain. Low back pain is a common condition in the elderly population, which often has a prolonged course, and is difficult to treat. Common causes of low back pain include lumbar spinal canal stenosis, intervertebral foramen stenosis, and lumbar disc herniation. A chronic compression of dorsal root ganglion (CCD)-induced neuropathic pain model in murine has been developed and applied in

¹Department of Physiology and Pathophysiology, School of Basic Medical Sciences, Xi'an Jiaotong University Health Science Center, Xi'an, PR China

²Key Laboratory of Environment and Genes Related to Diseases, Xi'an Jiaotong University, Ministry of Education, Beijing, PR China

³Department of Pain Medicine, Tianjin Union Medical Center, Nankai University, Tianjin, PR China

Corresponding Authors:

Jun Zhang, Department of Pain Medicine, Tianjin Union Medical Center, Nankai University, 190 Jieyuan Street, Tianjin 300121, PR China.
Email: doctor.zhangjun@hotmail.com

Lingli Liang, Department of Physiology and Pathophysiology, School of Basic Medical Sciences, Xi'an Jiaotong University Health Science Center, 76 Yanta Avenue, Xi'an, Shaanxi 710061, PR China.

Email: ll2017@xjtu.edu.cn



experimental studies for many years to mimics clinical intervertebral foramen stenosis and its related lumbocervical pain.¹⁻³

Tyrosine kinase receptor AXL belongs to the TYRO3, AXL and MERTK (TAM) tyrosine kinase receptor family, which plays roles in neural development and several neurological diseases. Growth arrest-specific protein 6 (GAS6) is the sole receptor for AXL.⁴ Soluble AXL (s-AXL), which only contains the extracellular domain of the full-length receptor of AXL, exists in murine and human plasma.^{5,6} S-AXL binds Gas6 and acts as a ligand sink to inhibit the normal cellular functions of full-length AXL receptor.^{5,6} Recent clinical studies have indicated that AXL might also be involved in pathological pain. One study showed that both s-AXL and GAS6 concentrations were increased in critical limb ischemia patients and correlated with levels of C-reactive protein, interleukin-6, tumor necrosis factor alpha, and neopterin.⁷ Another clinical study of patients with endometriosis also showed increased local AXL expression compared to a healthy control group.⁸ However, it remains unclear whether altered AXL activity in these two clinical pain conditions mediates pain symptoms.

GAS6/AXL may activate several intracellular signaling pathways that are involved in cell survival and proliferation, immunomodulation, myelination, synapse plasticity, as well as in other activities.⁹⁻¹¹ GAS6-activated AXL is involved in cell migration and survival via the intracellular phosphoinositide 3 kinase (PI3K)/protein kinase B (Akt) or the extracellular signal-regulated kinase signaling pathways.⁹ Multiple studies have shown that the PI3K/Akt signaling pathway contributes to the development of chronic pain.¹²⁻¹⁴ Mammalian target of rapamycin (mTOR) is a downstream target of PI3K/Akt that is also involved in morphine tolerance and neuropathic pain development.¹⁵⁻¹⁷ Therefore, AXL might contribute for activating cellular PI3K/Akt/mTOR signaling pathway in neuropathic pain development.

To explore the potential role of AXL in the neuropathic pain, we first examined expression changes of AXL mRNA and protein (activated AXL and total AXL) in the dorsal root ganglion (DRG) and spinal cord in rat neuropathic pain models. Second, we observed whether AXL inhibitor or AXL small interfering RNA (siRNA) relieved CCD-induced pain hypersensitivities. Finally, we examined whether mTOR signaling mediated the function of AXL in the DRG.

Materials and methods

Animals

Three- to four-week-old Sprague Dawley (SD) rats were served as donors for the DRG cell culture, and adult

male SD rats weighing 200 to 250 g were used for the remaining experiments of this study. All animals were housed in groups of three or four under a 12:12-h light/dark cycle with water and food available ad libitum. All procedures and animal housing facilities were approved by the Institutional Animal Ethics Committee of the Xi'an Jiaotong University Health Science Center and were conducted in accordance with the ethical guidelines of the International Association for the Study of Pain. Accordingly, efforts were made to minimize animal suffering as well as the number of animals used.

Neuropathic pain models

Spinal nerve ligation (SNL) surgery was performed using an existing procedure.^{18,19} Briefly, the lumbar 5 (L5) spinal nerve was exposed, ligated, and transected under 2.5% isoflurane anesthesia. The rats in the control, sham-surgery group underwent the identical surgical procedure without nerve ligation and transection.

CCD surgery was also carried out according to a previously described procedure.^{1,2} Under 2.5% isoflurane anesthesia, the L4 and L5 intervertebral foramina were exposed, and two L-shaped stainless steel rods (4 mm in length and 0.6 mm in diameter) were carefully inserted into the foramen and left there to compress the L4 and L5 DRGs, respectively. The stainless steel rods were not inserted into the intervertebral foramen in the sham-surgery receiving control group.

DRG cell culture and siRNA transfection

The DRGs of three- to four-week-old SD rats were harvested and subsequently cultured for assessment of the knockdown efficiency of AXL siRNA. In detail, the harvested DRGs were digested with 0.25% trypsin solution without EDTA (Beyotime Biotechnology, Shanghai, China) after being cut into pieces with a size that allowed their passage through the tip of a 1000 μ L pipettor. The digested cells were fully separated by repetitive (25 \times) blowing with a 1000 μ L pipettor, passed through a 70- μ m cell strainer, and then cultured in prewarmed NeurobasalTM-A Medium (Gibco/ThermoFisher Scientific, Waltham, MA) with 10% fetal bovine serum (JR Scientific, Woodland, CA), B-27TM Supplement (1 \times) (Gibco/ThermoFisher Scientific), 100 units/mL penicillin, and 100 μ g/mL streptomycin (Beyotime Biotechnology) in a six-well plate precoated with 50 μ g/mL poly-D-lysine (Beyotime Biotechnology). The cells were incubated in an incubator (37°C; 95% O₂, 5% CO₂). After a 24-h incubation, AXL siRNA (250 pmol) or equivalent negative control (NC) siRNA was added in Lipo6000 transfection reagent (Beyotime Biotechnology) to each well. AXL siRNA (5'-GCAUGCUGAAUGA

GAACAUTT-3'; 5'-AUGUUCUCAUUCAGCAUGC TT-3') and NC siRNA (5'-UUCUCCGAACGUG UCACGUTT-3'; 5'-ACGUGACACGUUCGGAGAA TT-3') were designed and synthesized by Genepharma (Shanghai, China). Two days later, the cultured cells were harvested in radio-immunoprecipitation assay (RIPA) lysis buffer for Western blotting.

Intrathecal catheter implantation and drug administration

The procedure for intrathecal catheter implantation for drug delivery has been previously described by us in detail.²⁰ Briefly, under 2.5% isoflurane anesthesia, a polyethylene-10 catheter was inserted into the subarachnoid space of the spinal cord. Ten microliters of siRNA, AXL inhibitor, or vehicle were injected into the catheter followed by a small air bubble and 10 μ L of sterile saline. Any rats showing postoperative neurologic deficits, such as hind-paw paralysis, were excluded from the study.

Intrathecal TP0903 (HY12963; MedChem Express, Shanghai, China) or vehicle (20% dimethyl sulfoxide) was administered 1 h before CCD surgery and then daily, from day 1 through day 5 post-CCD, TP0903 was injected intrathecally at three different doses (0.05, 0.50, and 1.00 μ g). Daily doses of intrathecal AXL siRNA, NC siRNA, or vehicle control (phosphate buffer saline) were administered starting on day 3 post-CCD, for a period of five days. Lipo6000 transfection reagent (Beyotime Biotechnology) was used as a vehicle for siRNA to improve delivery efficacy and to avoid siRNA degeneration.^{21,22}

Behavioral testing

During behavioral tests, pain behaviors in response to mechanical stimuli, noxious heat, and cold stimuli were tested similarly as in our previous studies.^{18,19,23} Paw-withdrawal thresholds (PWTs) in response to mechanical stimuli were measured using the up-down testing paradigm.^{24,25} To this end, each unrestrained rat was placed in a Plexiglass chamber on an elevated mesh screen after adaptation to the experimental environment. Calibrated von Frey filaments in log increments of force (0.41, 0.69, 1.20, 2.04, 3.63, 5.50, 8.51, 15.14, and 26.0 g) were applied onto the plantar surface of the rat's hind paws. The 2.04-g stimulus was applied first. If a positive response occurred, the next, smaller von Frey filament was used; if not, the next larger filament in the series was applied. The test was stopped when (1) a negative response to the 26.0-g filament was observed or (2) after the delivery of three more stimuli following the first positive response. The PWT was calculated using the formula provided by Dixon, that is, by

converting the pattern of positive and negative responses to a 50% threshold value.^{24,25}

Paw-withdrawal latencies (PWLs) to noxious heat stimuli were measured with a Model 37370 Analgesic Meter (UGO, Italy).^{19,23} Rats were placed on a glass plate within a Plexiglas chamber. Radiant heat stimuli were applied by a light beam to the middle of the plantar surface of each hind paw. The light beam was turned off automatically once rats showed a strong paw-withdrawal response. A stimulus cutoff time of 20 s was used to avoid tissue damage to paw. The PWL was defined as the evolved time between the start of the light beam and paw-withdrawal response. Five tests were performed at 10-min intervals for all paws, and an average PWL value was calculated for each paw.

Cold hyperalgesia was measured using a model ZH-6C cold plate (Zheng-Hua Biologic, Anhui, China). The temperature of the cold plate (diameter: 19 cm) was set at 0°C. Individual rats were placed on the cold plate inside a cylindrical transparent Plexiglas chamber (height: 28 cm, diameter: 20 cm). The response latency was measured from the moment when rats were put into a chamber until they showed a quick and strong paw flinch. A cutoff time of 60 s was used to avoid tissue damage of the animals' paws. Each trial was repeated three times at 15-min intervals.

RNA extraction, reverse transcription, and quantitative real-time polymerase chain reaction

Rats were first anesthetized and then killed by decapitation, and both L4/L5 DRGs and L4/L5 spinal cord segments were harvested and placed into RNAlater stabilization solution (Thermo Scientific). Tissues were homogenized in a cold tissue homogenizer (Shanghai Jingxin, China), and RNA was extracted with the RNeasyTM RNA extraction kit (Beyotime Biotechnology). RNA concentrations were quantified using a NanoDrop spectrophotometer (Thermo Scientific). Five hundred nanogram of RNA was reverse-transcribed with oligo (dT) primers using the RevertAid First Strand cDNA Synthesis Kit (Thermo Scientific) according to the manufacturer's directions. Quantitative polymerase chain reaction (qPCR) was performed in a 20 μ L volume containing 20 ng of cDNA, 250 nM forward and reverse primers, and 10 μ L of BeyoFastTM SYBR Green qPCR Mix (Beyotime Biotechnology) using the AXL primer (forward: 5'-GACCTAGCTGCCAGGAAGT-3'; reverse: 5'-ACACGCTACTCTTGCTGGT-3') or glyceraldehyde 3-phosphate dehydrogenase (GAPDH) primer (forward: 5'-TCGGTGTGAACGGATTGGC-3'; reverse: 5'-TCCCATTCTCGGCCTTGACT-3') in a BIO-RAD CFX96 real-time PCR system (Bio-Rad Laboratories, Hercules, CA). The following cycle parameters were

applied: initial 3-min incubation at 95°C, followed by 40 cycles with 95°C for 10 s, 60°C for 30 s, and 72°C for 30 s. All results were normalized to those obtained for GAPDH, the internal control. Ratios of mRNA levels in the ipsilateral side to the contralateral side were calculated using the ΔCt method ($2^{-\Delta\text{Ct}}$).

Western blotting

The collected ipsilateral and contralateral L4/L5 DRGs and spinal dorsal horns were put into AllProtect™ Nucleic Acid and Protein Stabilization Reagent for Animal Tissue (Beyotime Biotechnology) and stored at -20°C for subsequent analysis. The tissues were homogenized with ice-cold RIPA lysis buffer (50 mM Tris, 150 mM NaCl, 1% NP-40, 0.25% sodium deoxycholate, 1 mM phenylmethylsulfonyl fluoride; pH 7.4) with a protease-/phosphatase-inhibitor cocktail (Beyotime Biotechnology) using a Shanghai Jingxin tissue homogenizer (Shanghai Jingxin). After the crude homogenate was centrifuged at 4°C for 15 min at 1000 g, the supernatants were collected to assess cytosolic protein levels. Protein concentrations were measured using a Bradford Protein Assay Kit (Beyotime Biotechnology). Equal sample amounts were heated for 5 min at 99°C and loaded onto an 8% sodium dodecyl sulfate-polyacrylamide electrophoresis separation gel. The proteins were then electrophoretically transferred onto a nitrocellulose membrane, and the membrane was blocked with 3% nonfat milk in Tris-buffered saline containing 0.1% Tween-20 and followed by primary and secondary antibodies incubations. The primary antibodies including rabbit anti-phosphorylated AXL (anti-p-AXL) (phosphor Tyr697, 1:1000; GeneTex, Irvine, CA), rabbit anti-AXL (1:1000; Bioss, Peking, China), rabbit anti-mTOR (1:1000; Cell Signaling Technology, Danvers, MA), and mouse anti- β -actin (1:2000; Santa Cruz Biotechnology, Santa Cruz, CA) were incubated overnight at 4°C. The secondary antibodies including horseradish peroxidase-conjugated antirabbit and antimouse secondary antibody (1:3000; EMD Millipore, Darmstadt, Germany) were incubated at 25°C for 2 h. The proteins on the membrane were detected using western peroxide reagent and luminol/enhancer reagent (Immobilon Western Chemiluminescent HRP Substrate; EMD Millipore) and visualized using the Champchemi System with SageCapture software (Sagecreation Service for Life Science, Beijing, China). The intensity of blots was quantified by NIH ImageJ software. Each blot from the targeted protein was normalized relative to the corresponding β -actin blot. The average value of the control groups was set as 100% after normalization. The relative levels of the targeted protein at the different time points and/or the treated groups were determined by dividing the normalized

values from these groups by the average value of the control group.

Immunofluorescence

The L4/L5 DRGs were removed after transcatheter perfusion with 100 mL of perfusion buffer, followed by 250 mL of 4% paraformaldehyde in 0.1 M phosphate buffer. Subsequently, the tissues were postfixed, dehydrated, and then cut at 20 μm using a Leica CM3050 S cryostat. All DRG sections were placed directly on gelatin-covered slides. For single labeling of p-AXL, DRG sections were incubated overnight at 4°C with rabbit anti-p-AXL antibody (1:100; Genetex) after blocking with 10% normal goat serum. The sections were then incubated with goat antirabbit antibody conjugated to Alexa Fluor 488 (1:200; Abcam, Cambridge, MA) for 2 h at room temperature. For double labeling of p-AXL or AXL with DRG cell markers, DRG sections were incubated with rabbit anti-p-AXL antibody (1:100; Genetex) or anti-AXL antibody (1:200; Absin, Shanghai, China) and mouse anticalcitonin gene-related peptide (CGRP, 1:50; Abcam), mouse antineurofilament-200 (NF200, 1:500; Sigma, St. Louis, MO), or mouse antiglutamine synthetase (GS, 1:500; EMD Millipore), overnight at 4°C, followed by goat antirabbit antibody conjugated to Alexa Fluor 488 (1:200; Abcam) and goat antimouse antibody conjugated to Cy3 (1:200; Abcam) for 2 h at room temperature. For double labeling of p-AXL or AXL with biotinylated isolectin B4 (IB4, 1:100; Sigma), Alexa Fluor 488-conjugated goat antirabbit antibody (1:200; Abcam) and Cy3-conjugated Avidin (1:200; Abcam) were used as the second antibodies. The primary antiserum was omitted to obtain control DRG sections. The slides were coverslipped with SouthernBiotech Fluoromount-G (SouthernBiotech, Birmingham, AL) or antifade mounting medium with 4',6-diamidino-2-phenylindole (Beyotime Biotechnology). The single-labeled pictures were made by an Olympus BX53 fluorescence microscope, and double-labeled pictures were made using a Nikon C2 confocal microscope (Nikon, Tokyo, Japan). All pictures were quantified using NIH ImageJ Software.

Statistical analysis

The animals were randomly allocated to the various treatment groups. The number of rats was six per group in the behavioral, three per group in Western blotting, and five per group in immunofluorescence experiments. The data were statistically analyzed using SigmaPlot 12.5 software (San Jose, CA) by two-tailed, paired Student's *t* test for two-group comparisons, one-way analysis of variance (ANOVA) for comparisons of more than two groups, and two-way repeated measure

ANOVA for results from the behavioral tests. Whenever ANOVAs showed a significant difference, post hoc Tukey tests were performed for pairwise comparisons between means. All of the results were given as means \pm standard error of the mean. Tests yielding $P < 0.05$ were considered to be statistically significant.

Results

Increased AXL expression in injured DRGs

The expression and distribution of p-AXL and AXL in naive L4/L5 DRGs were examined by immunofluorescence (Figure 1(a)). Primary antibodies were omitted to obtain NC for p-AXL and AXL immunostaining (Figure 1(a)). Quantitative analysis showed that approximately $42.0 \pm 4.7\%$ of DRG neurons was positive for p-AXL and $51.8 \pm 4.0\%$ for AXL. All detectable p-AXL-positive neurons were small to medium ($<1200 \mu\text{m}^2$) in cross-sectional area. About 64.5% of

p-AXL-positive neurons were small ($<600 \mu\text{m}^2$) and the remaining were medium in size (Figure 1(b)). In all AXL-positive neurons, about 49.0% of them were small ($<600 \mu\text{m}^2$), 35.5% were medium ($<1200 \mu\text{m}^2$), and 15.4% were large in cross-sectional area (Figure 1(c)). Usually, NF200 was used to label medium/large neurons with myelinated A-fibers, CGRP for small DRG peptidergic neurons, and IB4 for small nonpeptidergic DRG neurons.^{26,27} Examination of the expression and distribution of p-AXL in naive L4/L5 DRGs by double-labeling immunofluorescence with NF200, CGRP, or IB4 (Figure 1(d)) demonstrated that p-AXL was dominantly expressed in IB4- or CGRP-positive DRG neurons. Of the p-AXL-positive neurons, $72.7 \pm 3.6\%$ showed colocalization with IB4 and $30.3 \pm 2.5\%$ with CGRP. None of the p-AXL-positive DRG neurons were NF200-positive (Figure 1(d); Table 1). However, AXL was colocalized not only with IB4 and CGRP but also with NF200 in naive L4/L5 DRGs (Figure 1(e)). Approximately $45.0 \pm 5.1\%$ of AXL-positive

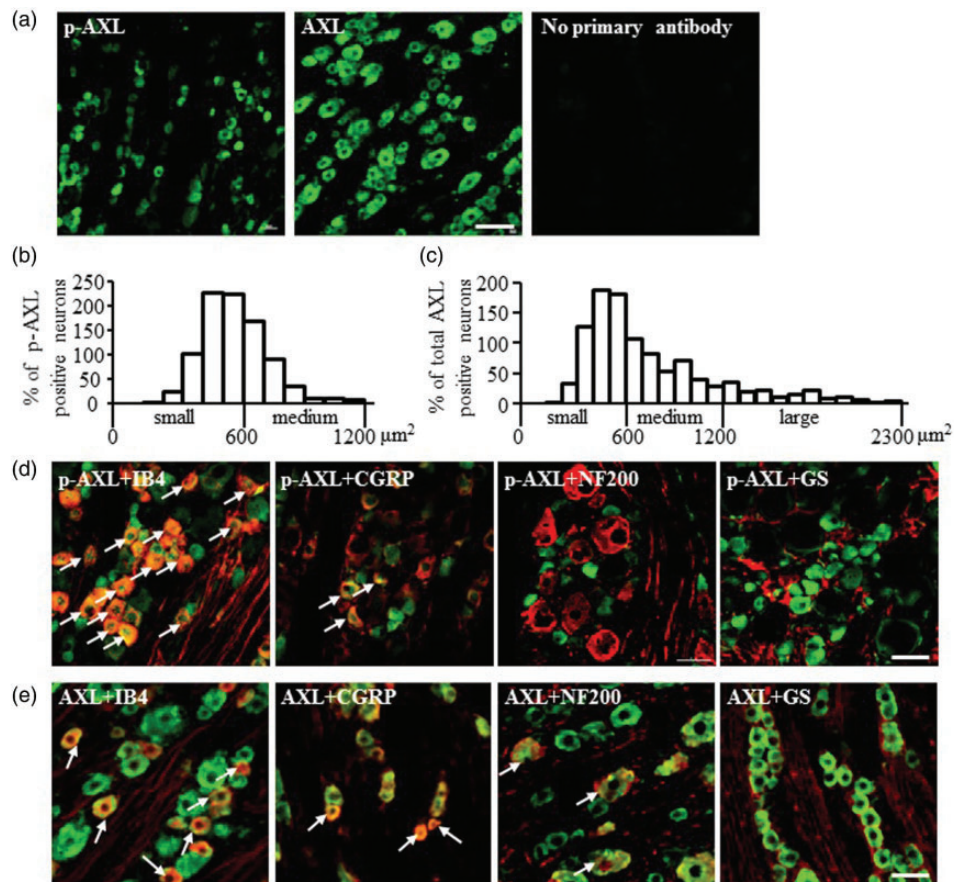


Figure 1. Expression of p-AXL and AXL in DRG. (a) The expression of p-AXL, AXL, and negative control without primary antibodies in naive L4/L5 DRGs. Histogram shows the distribution of p-AXL (b) and AXL (c) somata in naive L4/L5 DRGs. $N = 3$ rats, 6 to 8 slices per rat. (d) The colocalization of p-AXL with IB4, CGRP, NF200, or GS. (e) The colocalization of AXL with IB4, CGRP, NF200, or GS. Arrows: examples of double-labeled neurons. Scale bars: 100 μm (a); 25 μm (c and d). IB4: isolectin B4; CGRP: calcitonin gene-related peptide; NF200: neurofilament-200; p-AXL: phosphorylated AXL; GS: glutamine synthetase.

neurons were colocalized with IB4, $26.7 \pm 5.6\%$ with CGRP, and $27.5 \pm 3.7\%$ with NF200 (Figure 1(e); Table 1). Moreover, by using GS as the marker for DRG satellite glial cells,^{18,21} neither p-AXL nor AXL was detected in DRG satellite glial cells (Figure 1(d) and (e)).

Next, we examined the changes of p-AXL and AXL expression in neuropathic pain models. AXL mRNA levels were increased in injured DRGs in both SNL-

Table 1. The percentage of p-AXL- and AXL-positive neurons in three DRG neuron types (IB4-, CGRP-, or NF200-positive DRG neuron).

	IB4	CGRP	NF200
p-AXL	$72.7 \pm 3.6\%$	$30.3 \pm 2.5\%$	0
AXL	$45.0 \pm 5.1\%$	$26.7 \pm 5.6\%$	$27.5 \pm 3.7\%$

IB4: isolectin B4; CGRP: calcitonin gene-related peptide; NF200: neurofilament-200; p-AXL: phosphorylated AXL.

and CCD-induced neuropathic pain rats. In SNL rats, AXL mRNA in injured DRGs increased to 2.86-fold levels relative to the sham group on day 7 after surgery ($P < 0.01$, Figure 2(a)). In CCD rats, AXL mRNA increased to 3.21, 3.12, and 4.91-fold levels in compressed DRGs on days 3, 7, and 14, respectively ($F_{(3,15)} = 9.13$, $P < 0.01$, Figure 2(b)). Both p-AXL and AXL protein levels were increased significantly on days 7 and 14 ($F_{(3,15)} = 9.13$, $P < 0.01$) but not on day 3 after CCD surgery (Figure 2(c)). The ratio of p-AXL to AXL was increased only on day 7 after surgery (Figure 2(c)). The expression levels of p-AXL and AXL were unaltered in the contralateral DRGs or the ipsilateral spinal cord at any of the examined time points (Figure 2(d) and (e)). Accordingly, the percentage of p-AXL-positive neurons and AXL-positive neurons in compressed DRGs was increased by 13.2% and 13.9%, respectively, relative to that of sham-operated DRGs ($55.2 \pm 5.3\%$ vs. $42.0 \pm 4.7\%$, $P < 0.01$, Figure 3(a) and (b); $65.7 \pm 4.3\%$ vs. $51.8 \pm 4.0\%$, $P < 0.01$, Figure 3(c) and (d)).

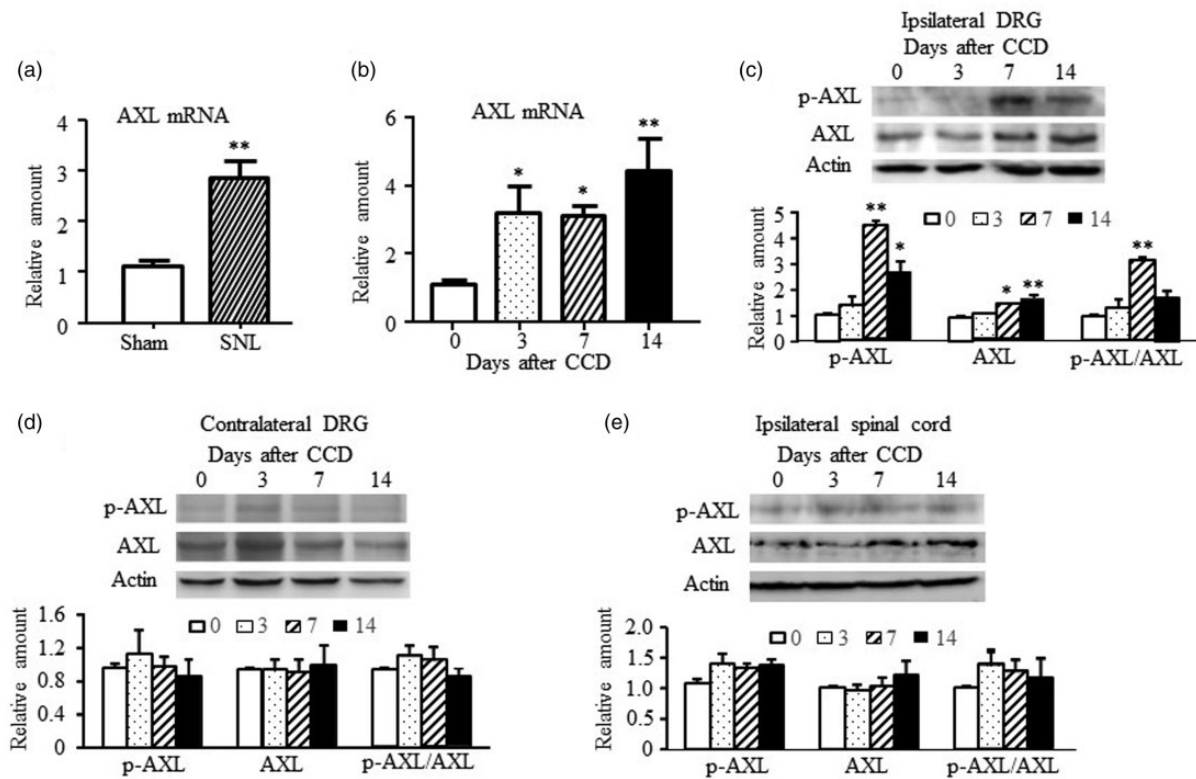


Figure 2. Expression changes of AXL mRNA and AXL protein in the DRG and spinal dorsal horn in neuropathic pain models. (a) The amount of AXL mRNA was increased in the ipsilateral L5 DRG on day 7 in the SNL-induced neuropathic pain model. $N = 5$ rats per group. $**P < 0.01$ versus the sham group by two-tailed unpaired Student's *t* test. (b) The amount of AXL mRNA was increased in the ipsilateral L4/L5 DRG on days 3, 7, and 14 in CCD-induced neuropathic pain model. $N = 3$ or 4 rats/time point. One-way ANOVA (expression vs. time points) followed by post hoc Tukey tests, $*P < 0.05$, $**P < 0.01$ versus day 0 (sham group). (c) The protein amount of p-AXL and total AXL increased in the ipsilateral L4/L5 DRGs after CCD surgery. $N = 3$ or 4 rats/time point. One-way ANOVA (expression vs. time points) followed by post hoc Tukey test, $*P < 0.05$, $**P < 0.01$ versus day 0 (sham group). No significant changes in p-AXL and total AXL were observed in the contralateral L4/L5 DRGs (d) and the ipsilateral L4/L5 spinal dorsal horns (e) at all observed time points after CCD surgery. DRG: dorsal root ganglion; CCD: chronic compression of DRG; SNL: spinal nerve ligation; p-AXL: phosphorylated AXL.

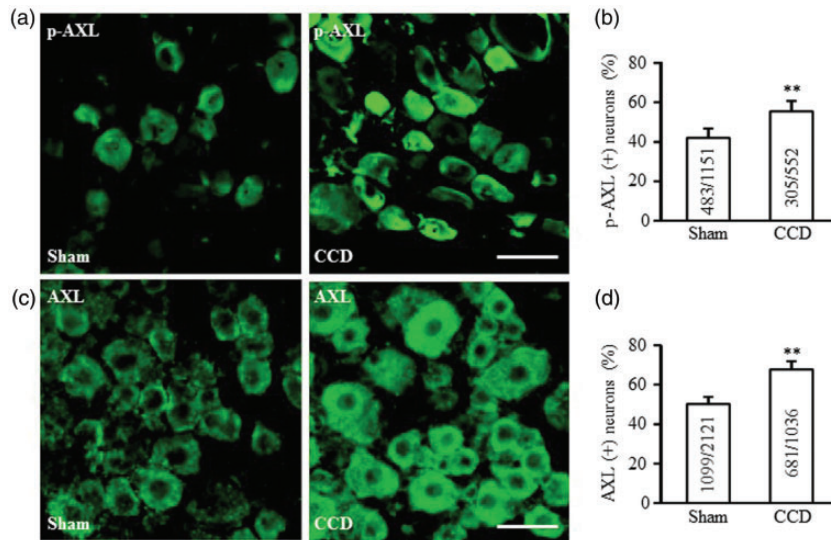


Figure 3. Expression changes of p-AXL- and AXL-positive neurons in the DRG in CCD-induced neuropathic pain model. (a and b) The percentage of p-AXL-positive (+) neurons increased in compressed L4/L5 DRGs of CCD rats. The value on each histogram shows the ratio of p-AXL (+) neurons to total counted neurons in DRG slices. $N = 5$ rats/group. $**P < 0.01$ versus the sham group by two-tailed unpaired Student's t test. (c and d) The percentage of AXL-positive (+) neurons increased in compressed L4/L5 DRGs of CCD rats. The value on each histogram shows the ratio of AXL (+) neurons to total counted neurons in DRG slices. $N = 3$ rats/group. $**P < 0.01$ versus the sham group by two-tailed unpaired Student's t test. Scale bar: $50 \mu\text{m}$.

CCD: chronic compression of dorsal root ganglion; p-AXL: phosphorylated AXL.

Inhibition of AXL activation attenuates CCD-induced pain hypersensitivities

Increases in the p-AXL/AXL ratio indicate a potential role of AXL receptor activation in the pathological mechanisms induced by DRG compression. We used a selective and effective AXL receptor inhibitor TP0903 to assess whether AXL mediated CCD-induced neuropathic pain. It has been reported that CCD could induce mechanical and thermal pain hypersensitivities as early as day 2 and last for over 35 days.¹⁻³ We observed the effect of repeated TP0903 (0.05, 0.50, or 1.00 μg) on CCD induced the changes in paw-withdrawal responses to mechanical, thermal, and cold stimuli on days 4 and 6 post-CCD. TP0903 or vehicle solution was intrathecally administered 1 h before CCD or sham surgery and once daily for five days after CCD or sham surgery. On days 4 and 6, ipsilateral PWTs to mechanical stimuli, PWLs to thermal stimuli, and response latencies to cold stimuli in the CCD plus vehicle group were decreased significantly compared to the sham-operation plus vehicle group (Figure 4(a)). Repeated injections of 0.50 and 1.00 μg TP0903 reversed these decreases in latency (Figure 4(a) to (c)). Also on days 4 and 6 after CCD surgery, PWTs to mechanical, PWLs to thermal, and positive response latencies to cold stimulation were much higher on the ipsilateral side of the TP0903 plus CCD group than in the CCD plus vehicle group (Figure 4(a): $F_{(15,191)} = 10.38$, Figure 4(b): $F_{(15,191)} = 7.33$, Figure 4

(c): $F_{(15,191)} = 16.96$, $**P < 0.01$, vs. Sham + Veh, $###P < 0.01$, vs. CCD + Veh). The 0.05 μg dose of TP0903 did not affect the CCD-induced decreases in paw-withdrawal responses (Figure 4(a) to (c)). Moreover, the 1 μg dose of TP0903 did not alter basal paw-withdrawal responses to mechanical, thermal, and cold stimuli in sham-operated rats ($P > 0.05$, Figure 4(a) to (c)). These results indicate that the AXL inhibitor, TP0903, exhibited analgesic effects on CCD-induced pain hypersensitivities to mechanical, thermal, and cold stimuli.

Knockdown of DRG AXL relieves CCD-induced pain hypersensitivities

In order to assess the relationship between total AXL-protein expression and neuropathic pain, we examined the effect of DRG AXL knockdown on CCD-induced pain hypersensitivities in rats by intrathecally administering AXL siRNA. First, the knockdown efficiency of AXL siRNA was confirmed in vitro by DRG cell culture. As shown in Figure 5(a), transfection of AXL siRNA (125 nM) was associated with a 50% decrease in total AXL expression relative to NC siRNA treatment ($P < 0.01$). In the subsequent in vivo experiment, AXL siRNA or NC siRNA was administered intrathecally once daily for five days starting on day 3 postsurgery. As expected, AXL expression increased significantly in ipsilateral L4/L5 DRGs in the CCD plus vehicle group.

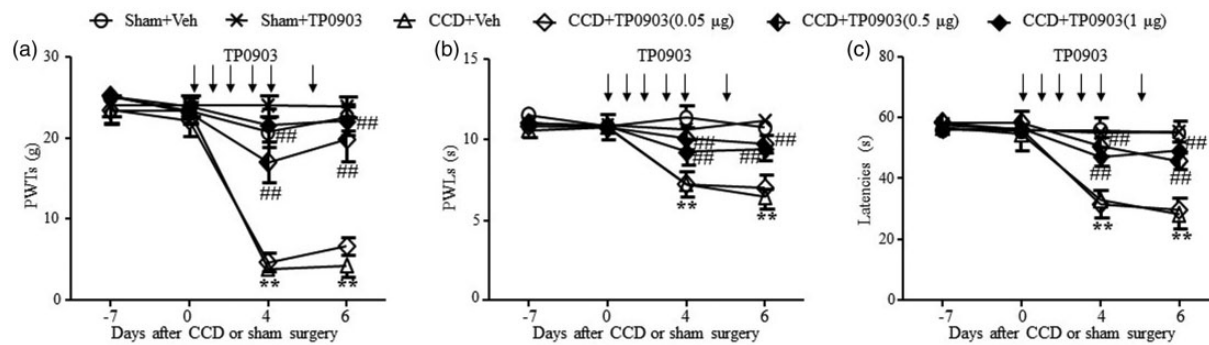


Figure 4. Effects of AXL inhibitor TP903 on CCD-induced nociceptive hypersensitivities. The dose of TP903 (0.05, 0.5, or 1 μg) or vehicle solution was intrathecally administered 1 h before CCD or sham surgery and once daily for five days after CCD or sham surgery. The doses of 0.5 and 1 μg inhibited (a) the decrease of PWTs to mechanical stimulation, (b) PWLs to thermal stimulation, and (c) positive response latencies to cold stimulation on the ipsilateral side of CCD rats. $N = 6$ rats/group. Two-way repeated measure ANOVA (effect vs. group \times time interaction) followed by post hoc Tukey tests, $**P < 0.01$ versus the corresponding time point in the Sham + Veh group. $###P < 0.01$ versus the corresponding time point in the CCD + Veh group.

PWT: paw-withdrawal threshold; PWL: paw-withdrawal latency; CCD: chronic compression of dorsal root ganglion.

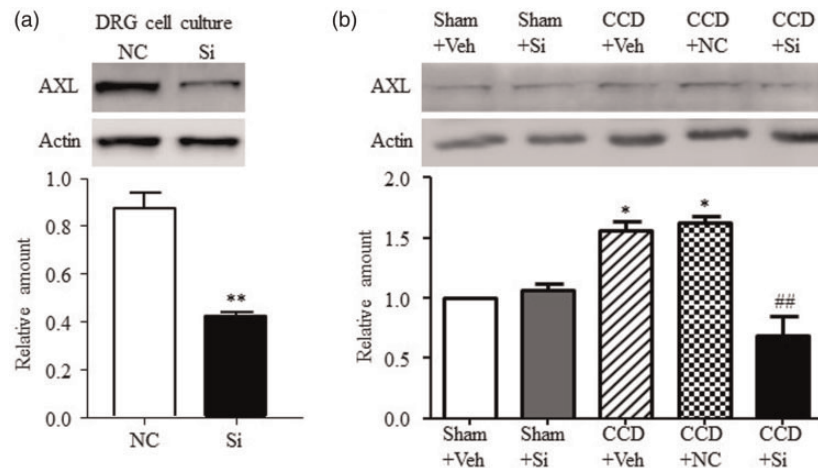


Figure 5. AXL siRNA suppressed AXL expression in vitro and in vivo. (a) The amount of AXL was markedly decreased by AXL siRNA (Si, 250 nM) treatment in DRG cell culture. $N = 3$ repeats (six wells from three rats) per treatment. $**P < 0.01$ versus NC siRNA by two-tailed unpaired Student's t test. (b) Intrathecal injection of AXL siRNA (10 μM in 10 μL) blocked the increase of AXL induced by CCD and did not affect the basal level of AXL in the sham group. The first injection was administered on day 3 post-CCD and repeated once daily for five days, and ipsilateral L4/L5 DRGs were harvested on day 8 post-CCD. $N = 3$ rats/time point. One-way ANOVA (effect vs. the treated groups) followed by post hoc Tukey tests, $*P < 0.05$ versus the Sham + Veh group. $###P < 0.01$ versus the CCD + Veh group. NC: negative control; DRG: dorsal root ganglion; CCD: chronic compression of DRG.

AXL siRNA (5 μM /10 μL), but not NC siRNA (5 μM /10 μL), reversed the upregulation of CCD-induced AXL expression in the ipsilateral compressed L4/L5 DRGs ($F_{(4,19)} = 21.67$, $**P < 0.01$ vs. Sham + Veh, $###P < 0.01$ vs. CCD + Veh; Figure 5(b)). However, the basal expression of AXL in the ipsilateral L4/L5 DRGs was not affected by AXL siRNA in the sham plus AXL siRNA group compared with the sham plus vehicle group (Figure 5(b)). This result, which we also found in previous studies,^{18,21} may be due to a low expression level of target genes in the basal condition.

All paw-withdrawal responses were tested on days 6 and 8 after sham or CCD surgery. PWTs to mechanical stimulation, PWLs to thermal stimulation, and positive latencies to cold stimulation were significantly decreased on the ipsilateral side in the CCD plus vehicle group ($**P < 0.01$, vs. Sham + Veh, Figure 6(a) to (c)). These decreases were reversed by repeated intrathecal injection of AXL siRNA (Figure 6(a): $F_{(8,119)} = 25.20$, Figure 6(b): $F_{(8,119)} = 32.92$, Figure 6(c): $F_{(8,119)} = 29.99$, $###P < 0.01$, vs. CCD + Veh) but not by NC siRNA administration ($P > 0.05$, Figure 6(a) to (c)). Neither

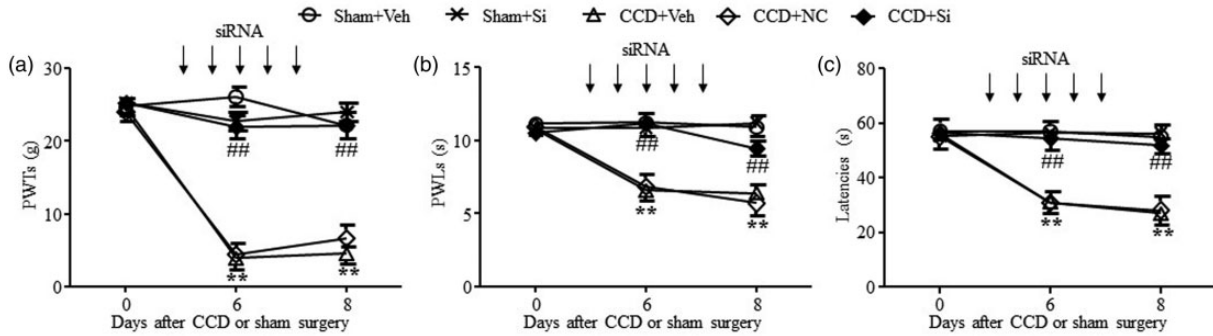


Figure 6. Effect of AXL siRNA on CCD-induced nociceptive hypersensitivities. All siRNAs ($10 \mu\text{M}$ in $10 \mu\text{L}$ vehicle solution) or vehicle solutions were intrathecally administered from day 3 to day 7 once daily for five days. Intrathecal injection of AXL siRNA (Si) but not NC siRNA reversed the decrease of PWTs to mechanical stimulation (a), PWLs to thermal stimulation (b), or positive response latencies to cold stimulation (c) on the ipsilateral side of CCD rats. $N=6$ rats/group. Two-way repeated measure ANOVA (effect vs. group \times time interaction) followed by post hoc Tukey tests. $**P < 0.01$ versus the corresponding time point in the Sham + Veh group. $###P < 0.01$ versus the corresponding time point in the CCD + Veh group. NC: negative control; PWT: paw-withdrawal threshold; PWL: paw-withdrawal latency; CCD: chronic compression of dorsal root ganglion; siRNA: small interfering RNA.

AXL siRNA nor NC siRNA changed the basal level of paw-withdrawal responses to mechanical, thermal, or cold stimuli (Figure 6(a) to (c)). These results suggested a potential role of both activated AXL and total AXL in CCD-induced pain hypersensitivity.

mTOR mediates the intracellular effect of AXL

We found that the expression of AXL in injured DRGs was upregulated in rats with CCD-induced neuropathic pain, and intracellular mTOR signaling participated in the peripheral mechanism underlying neuropathic pain. Specifically, p-AXL was primarily located on IB4-positive neurons and CGRP-positive neurons in DRG. Inhibition of AXL activity, or interference of AXL expression in DRG, can effectively alleviate pain sensitivities in CCD rats. While previous studies have indicated that AXL activated the PI3K/Akt signaling pathway,⁹ we examined whether AXL activated, or otherwise influenced, mTOR signaling, a downstream target of PI3K/Akt that is involved in morphine tolerance and neuropathic pain development.^{15–17} Our previous work have shown that mTOR expression increased in the compressed DRGs after CCD surgery.²⁸ We further confirmed that the expression of phosphorylated mTOR (p-mTOR) and total mTOR increased in ipsilateral DRGs on day 7 and day 14 (p-mTOR: $F_{(3,11)}=7.40$, $P < 0.05$; mTOR: $F_{(3,11)}=14.93$, $P < 0.01$) but not on day 3 after CCD surgery (Figure 7(a)). The ratio of p-mTOR to mTOR does not change at any detected time points (Figure 7(a)), suggesting that the change of mTOR activation is totally due to the increased total mTOR protein. Daily intrathecal injection of either TP0903 ($1 \mu\text{g}$ per day; Figure 7(b)) or AXL siRNA ($5 \mu\text{M}$ in $10 \mu\text{L}$ vehicle solution per day; Figure 7(c)) reversed the increase of p-mTOR (Figure 7(b):

$F_{(2,13)}=12.8$, $P < 0.01$; Figure 7(c): $F_{(2,13)}=12.2$, $P < 0.01$) and mTOR expression (Figure 7(b): $F_{(2,13)}=16.9$, $P < 0.01$; Figure 7(c): $F_{(2,13)}=17.0$, $P < 0.01$) in CCD rats. However, the ratio of p-mTOR to mTOR does not change at any treated groups compared with the sham plus vehicle group. This result suggests that AXL enhanced mTOR signaling, thus involved in peripheral mechanisms of neuropathic pain.

Discussion

In this study, p-AXL was found to be located mainly on IB4-positive neurons and CGRP-positive neurons, as demonstrated by immunofluorescence double labeling. This indicates a potential role of AXL in nociceptive signaling. We further found that spinal nerve or DRG injury induced upregulation of AXL expression in injured DRGs. Inhibition of AXL activity or interference of AXL expression in DRG effectively alleviated pain hypersensitivities induced by CCD surgery. Finally, the effect of AXL on CCD-induced neuropathic pain may be mediated by intracellular mTOR signaling.

AXL is a member of the TAM family of receptor tyrosine kinases, which also includes tyrosine kinase receptor 3 (Tyro3) and Mer.^{6,9} The TAM receptor family regulates normal cellular processes and plays important roles in the nervous system development and diseases, specifically in cell proliferation/survival, cell adhesion and migration, neuronal differentiation, cell apoptosis, myelination, degeneration, and immune regulation.^{6,9} However, it is not known whether TAM is involved in peripheral mechanisms of neuropathic pain. In a previous study by our group, RNA-Seq analysis of spinal nerve-ligated DRGs demonstrated a significant increase of AXL mRNA in injured L4 DRG in mice.²⁹ We further evaluated if AXL might be a potential target

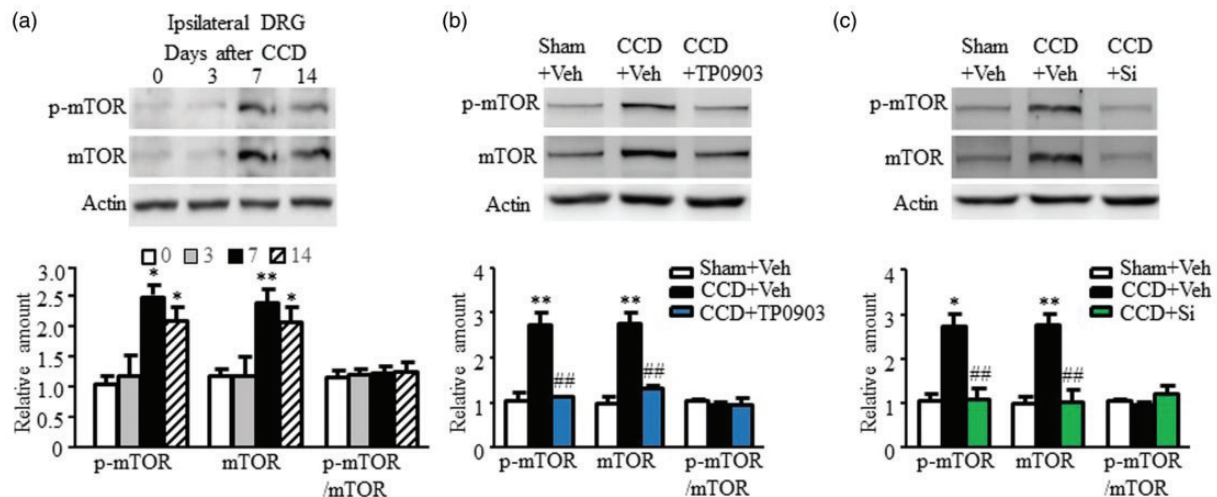


Figure 7. Mediation by the intracellular signaling molecule, mTOR, of nociceptive effects of AXL. (a) The protein amount of p-mTOR and total mTOR increased in the ipsilateral L4/L5 DRGs on days 7 and 14 after CCD surgery. $N = 3$ rats/time point. One-way ANOVA (expression vs. time points) followed by post hoc Tukey test, $*P < 0.05$, $**P < 0.01$ versus day 0 (sham group). Repeatedly intrathecal injection of (b) TP0903 (1 μg) or (c) AXL siRNA (Si, 5 μM in 10 μL vehicle solution) reduced mTOR expression in compressed DRGs of CCD rats. $N = 3$ rats/time point. One-way ANOVA (effect vs. the treated groups) followed by post hoc Tukey tests, $*P < 0.05$, $**P < 0.01$, versus the Sham + Veh group; $###P < 0.01$ versus the CCD + Veh group. DRG: dorsal root ganglion; CCD: chronic compression of DRG; mTOR: mammalian target of rapamycin.

for the treatment of neuropathic pain. First, the predominant expression of p-AXL and AXL in small-sized DRG neurons suggests a potential role of DRG AXL in nociceptive processes. Second, CCD induced the upregulation of both p-AXL and AXL in injured DRGs in SNL and CCD-induced neuropathic pain models. Inhibition of AXL activation or knockdown of AXL expression relieved CCD-induced pain hypersensitivities. This study provides preliminary evidence for the involvement of DRG AXL in the development of neuropathic pain.

In our study, both neuropathic pain models, SNL and CCD, were used to examine the expression of AXL in injured DRGs. Based on the previous reports,^{1–3,15,18} SNL caused DRG injury and pain hypersensitivities by ligation and transection of L5 spinal nerve in rats, while CCD caused DRG injury and pain hypersensitivities in rats by compressing L4 and L5 DRGs. Therefore, we conclude that the upregulation of AXL expression in injured DRGs is universal despite of injury types. It has been claimed that GAS6 is the sole ligand for AXL.³⁰ Although in our study, SNL or CCD upregulated the expression of AXL in injured DRGs, the transcriptional expression of GAS6 in sham and SNL groups was similar.²⁹ Interestingly, nerve growth factor (NGF) receptor, a well-known receptor tyrosine kinase that is involved in pathologic pain,^{31–33} regulates AXL expression in in vitro cytomegalovirus (CMV)-AXL-enhanced green fluorescent protein (EGFP) plasmid-transfected PC12 cells.³⁴ Moreover, NGF expression is increased

in injured DRGs in some models of animal neuropathic pain, for example, chronic constriction injury of sciatic nerve and spared nerve injury.^{31,32} Therefore, NGF may be a trigger for the increased expression of AXL. However, this requires further verification in future studies.

PI3K/Akt/mTOR is a classic intracellular pathway that is involved in multiple physical processes, including cell metabolism, proliferation, differentiation, and apoptosis.^{35–37} The PI3K/Akt/mTOR signaling pathway is implicated in peripheral and spinal mechanisms of inflammatory pain, neuropathic pain, cancer pain, and morphine tolerance.^{15–17} The expression of p-Akt was increased in the injured DRG and spinal dorsal horn of a preclinical neuropathic pain rat model with spinal nerve injury or sciatic nerve injury.^{14,20} Administration of PI3K or Akt inhibitors not only relieved pain hypersensitivities in these rats but also reversed the increase of p-Akt in the injured DRG and spinal dorsal horn.¹⁴ Increased levels of p-mTOR and unphosphorylated mTOR have been found in primary sensory afferents, DRG, and the spinal dorsal horn.¹⁶ In addition, rapamycin, an mTOR inhibitor, is known to attenuate nerve injury-induced pain hypersensitivities.^{14,17} Following up on previous studies showing that AXL activates the PI3K/Akt pathway,^{38–40} we further examined the effect of AXL intervention on mTOR expression and found that either DRG AXL inhibition or AXL knockdown decreased total mTOR expression in DRG. In the DRG, medium/large neurons with myelinated A-fibers are

generally labeled by NF200, small peptidergic DRG neurons by CGRP, and small nonpeptidergic DRG neurons by IB4.^{26,27,41} p-AXL, like p-Akt and p-mTOR,^{14,16} was found to be expressed in small-sized DRG neurons, especially in IB4-positive neurons, suggesting that PI3K/Akt/mTOR is an intracellular signaling pathway of the AXL receptor, which mediates neuropathic pain. However, Xu et al. has reported that the numbers of p-Akt positive neurons could increase as early as one day after SNL surgery.¹⁴ In this study, we observed a significant increase of AXL mRNA on day 3 after CCD, but no change of p-AXL and total AXL protein expression were observed at this time point. It is possibly due to that the PI3K/Akt/mTOR signaling pathway was activated by other activated receptors at initial three days after CCD and then by AXL at late time points.

In summary, this study demonstrates that nerve injury may increase AXL in injured DRGs in a CCD-induced neuropathic pain model, which mimics human intervertebral foramen stenosis of lumbocrustral pain. Both AXL inhibitor and AXL siRNA were found to reverse various CCD-induced pain hypersensitivities in rats. While some AXL inhibitors have already been validated in clinical trials for the treatment of tumors,⁴² AXL may also be considered as a potential therapeutic target for pain.

Author Contributions

LL designed experiments and wrote the manuscript. JZ generated idea and provided valuable advices on the research. LT, SW, and LX did Western blotting and immunohistochemistry experiments. YW, QG-S, YD, YC, HJ, XY, and CY did behavioral tests. All authors read and edited the manuscript.

Declaration of Conflicting Interests

The author(s) declared no potential conflicts of interest with respect to the research, authorship, and/or publication of this article.

Funding

The author(s) disclosed receipt of the following financial support for the research, authorship, and/or publication of this article: This work was supported by the Key Projects of National Health and Family Planning Commission of Tianjin, China (16KG157), the National Natural Science Foundation of China (81701112 and 31871065), the Natural Science Foundation of Shaanxi Province (2019JM-128), and the China Postdoctoral Science Foundation (2018M633527).

ORCID iD

Lingli Liang  <https://orcid.org/0000-0001-7594-387X>

References

- Hu SJ, Xing JL. An experimental model for chronic compression of dorsal root ganglion produced by intervertebral foramen stenosis in the rat. *Pain* 1998; 77: 15–23.
- Xie Y-B, Zhao H, Wang Y, Song K, Zhang M, Meng F-C, Yang Y-J, He Y-S, Kuang F, You S-W, You H-J, Xu H. Bilateral neuropathy of primary sensory neurons by the chronic compression of multiple unilateral DRGs. *Neural Plast* 2016; 2016: 2130901.
- Wang T, Hurwitz O, Shimada SG, Qu L, Fu K, Zhang P, Ma C, LaMotte RH. Chronic compression of the dorsal root ganglion enhances mechanically evoked pain behavior and the activity of cutaneous nociceptors in mice. *PLoS One* 2015; 10: e0137512.
- Binder MD, Kilpatrick TJ. TAM receptor signalling and demyelination. *Neurosignals* 2009; 17: 277–287.
- Budagian V, Bulanova E, Orinska Z, Duitman E, Brandt K, Ludwig A, Hartmann D, Lemke G, Saftig P, Bulfone-Paus S. Soluble Axl is generated by ADAM10-dependent cleavage and associates with Gas6 in mouse serum. *Mol Cell Biol* 2005; 25: 9324–9339.
- Zhang J, Qi X. The role of the TAM family of receptor tyrosine kinases in neural development and disorders. *Neuropsychiatry (Lond)* 2017; 7: 729–732.
- Ekman C, Gottsater A, Lindblad B, Dahlback B. Plasma concentrations of Gas6 and soluble Axl correlate with disease and predict mortality in patients with critical limb ischemia. *Clin Biochem* 2010; 43: 873–876.
- Honda H, Barreto FF, Gogusev J, Im DD, Morin PJ. Serial analysis of gene expression reveals differential expression between endometriosis and normal endometrium. Possible roles for AXL and SHC1 in the pathogenesis of endometriosis. *Reprod Biol Endocrinol* 2008; 6: 59.
- Pierce AM, Keating AK. TAM receptor tyrosine kinases: expression, disease and oncogenesis in the central nervous system. *Brain Res* 2014; 1542: 206–220.
- Keating AK, Kim GK, Jones AE, Donson AM, Ware K, Mulcahy JM, Salzberg DB, Foreman NK, Liang X, Thorburn A, Graham DK. Inhibition of Mer and Axl receptor tyrosine kinases in astrocytoma cells leads to increased apoptosis and improved chemosensitivity. *Mol Cancer Ther* 2010; 9: 1298–1307.
- Zagorska A, Traves PG, Lew ED, Dransfield I, Lemke G. Diversification of TAM receptor tyrosine kinase function. *Nat Immunol* 2014; 15: 920–928.
- Man H-Y, Wang Q, Lu W-Y, Ju W, Ahmadian G, Liu L, D'Souza S, Wong TP, Taghibiglou C, Lu J, Becker LE, Pei L, Liu F, Wymann MP, MacDonald JF, Wang YT. Activation of PI3-kinase is required for AMPA receptor insertion during LTP of mEPSCs in cultured hippocampal neurons. *Neuron* 2003; 38: 611–624.
- Sui L, Wang J, Li BM. Role of the phosphoinositide 3-kinase-Akt-mammalian target of the rapamycin signaling pathway in long-term potentiation and trace fear conditioning memory in rat medial prefrontal cortex. *Learn Mem* 2008; 15: 762–776.
- Xu JT, Tu HY, Xin WJ, Liu XG, Zhang GH, Zhai CH. Activation of phosphatidylinositol 3-kinase and protein kinase B/Akt in dorsal root ganglia and spinal cord

- contributes to the neuropathic pain induced by spinal nerve ligation in rats. *Exp Neurol* 2007; 206: 269–279.
15. Liang L, Tao B, Fan L, Yaster M, Zhang Y, Tao YX. mTOR and its downstream pathway are activated in the dorsal root ganglion and spinal cord after peripheral inflammation, but not after nerve injury. *Brain Res* 2013; 1513: 17–25.
 16. Xu JT, Zhao X, Yaster M, Tao YX. Expression and distribution of mTOR, p70S6K, 4E-BP1, and their phosphorylated counterparts in rat dorsal root ganglion and spinal cord dorsal horn. *Brain Res* 2010; 1336: 46–57.
 17. Xu JT, Sun L, Lutz BM, Bekker A, Tao YX. Intrathecal rapamycin attenuates morphine-induced analgesic tolerance and hyperalgesia in rats with neuropathic pain. *Transl Perioper Pain Med* 2015; 2: 27–34.
 18. Zhang J, Liang L, Miao X, Wu S, Cao J, Tao B, Mao Q, Mo K, Xiong M, Lutz BM, Bekker A, Tao Y-X. Contribution of the suppressor of variegation 3-9 homolog 1 in dorsal root ganglia and spinal cord dorsal horn to nerve injury-induced nociceptive hypersensitivity. *Anesthesiology* 2016; 125: 765–778.
 19. Zhao J-Y, Liang L, Gu X, Li Z, Wu S, Sun L, Atianjoh FE, Feng J, Mo K, Jia S, Lutz BM, Bekker A, Nestler EJ, Tao Y-X. DNA methyltransferase DNMT3a contributes to neuropathic pain by repressing *Kcna2* in primary afferent neurons. *Nat Commun* 2017; 8: 14712.
 20. Liang L, Fan L, Tao B, Yaster M, Tao YX. Protein kinase B/Akt is required for complete Freund's adjuvant-induced upregulation of Nav1.7 and Nav1.8 in primary sensory neurons. *J Pain* 2013; 14: 638–647.
 21. Li Z, Mao Y, Liang L, Wu S, Yuan J, Mo K, Cai W, Mao Q, Cao J, Bekker A, Zhang W. The transcription factor C/EBPbeta in the dorsal root ganglion contributes to peripheral nerve trauma-induced nociceptive hypersensitivity. *Sci Signal* 2017; 10: eaam5345.
 22. Otsuka S, Adamson C, Sankar V, Gibbs KM, Kane-Goldsmith N, Ayer J, Babiarz J, Kalinski H, Ashush H, Alpert E, Lahav R, Feinstein E, Grumet M. Delayed intrathecal delivery of RhoA siRNA to the contused spinal cord inhibits allodynia, preserves white matter, and increases serotonergic fiber growth. *J Neurotrauma* 2011; 28: 1063–1076.
 23. Li Z, Gu X, Sun L, Wu S, Liang L, Cao J, Lutz BM, Bekker A, Zhang W, Tao Y-X. Dorsal root ganglion myeloid zinc finger protein 1 contributes to neuropathic pain after peripheral nerve trauma. *Pain* 2015; 156: 711–721.
 24. Dixon WJ. Efficient analysis of experimental observations. *Annu Rev Pharmacol Toxicol* 1980; 20: 441–462.
 25. Chaplan SR, Bach FW, Pogrel JW, Chung JM, Yaksh TL. Quantitative assessment of tactile allodynia in the rat paw. *J Neurosci Methods* 1994; 53: 55–63.
 26. Liang L, Wang Z, Lu N, Yang J, Zhang Y, Zhao Z. Involvement of nerve injury and activation of peripheral glial cells in tetanic sciatic stimulation-induced persistent pain in rats. *J Neurosci Res* 2010; 88: 2899–2910.
 27. Yu L, Yang F, Luo H, Liu F-Y, Han J-S, Xing G-G, Wan Y. The role of TRPV1 in different subtypes of dorsal root ganglion neurons in rat chronic inflammatory nociception induced by complete Freund's adjuvant. *Mol Pain* 2008; 4: 61.
 28. Wang S, Liu S, Xu L, Zhu X, Liu W, Tian L, Chen Y, Wang Y, Nagendra BVP, Jia S, Liang L, Huo F-Q. The upregulation of EGFR in the dorsal root ganglion contributes to chronic compression of dorsal root ganglions-induced neuropathic pain in rats. *Mol Pain* 2019; 15: 1744806919857297.
 29. Wu S, Marie Lutz B, Miao X, Liang L, Mo K, Chang Y-J, Du P, Soteropoulos P, Tian B, Kaufman AG, Bekker A, Hu Y, Tao Y-X. Dorsal root ganglion transcriptome analysis following peripheral nerve injury in mice. *Mol Pain* 2016; 12: 174480691662904.
 30. Hoehn HJ, Kress Y, Sohn A, Brosnan CF, Bourdon S, Shafit-Zagardo B. *Axl*^{-/-} mice have delayed recovery and prolonged axonal damage following cuprizone toxicity. *Brain Res* 2008; 1240: 1–11.
 31. Wu J-R, Chen H, Yao Y-Y, Zhang M-M, Jiang K, Zhou B, Zhang D-X, Wang J. Local injection to sciatic nerve of dexmedetomidine reduces pain behaviors, SGCs activation, NGF expression and sympathetic sprouting in CCI rats. *Brain Res Bull* 2017; 132: 118–128.
 32. Terada Y, Morita-Takemura S, Isonishi A, Tanaka T, Okuda H, Tatsumi K, Shinjo T, Kawaguchi M, Wanaka A. NGF and BDNF expression in mouse DRG after spared nerve injury. *Neurosci Lett* 2018; 686: 67–73.
 33. Yao P, Ding Y, Wang Z, Ma J, Hong T, Zhu Y, Li H, Pan S. Impacts of anti-nerve growth factor antibody on pain-related behaviors and expressions of opioid receptor in spinal dorsal horn and dorsal root ganglia of rats with cancer-induced bone pain. *Mol Pain* 2016; 12: 174480691664492.
 34. Wang Q, Lu QJ, Xiao B, Zheng Y, Wang XM. Expressions of *Axl* and Tyro-3 receptors are under regulation of nerve growth factor and are involved in differentiation of PC12 cells. *Neurosci Bull* 2011; 27: 15–22.
 35. Follo MY, Manzoli L, Poli A, McCubrey JA, Cocco L. PLC and PI3K/Akt/mTOR signalling in disease and cancer. *Adv Biol Regul* 2015; 57: 10–16.
 36. Yu JS, Cui W. Proliferation, survival and metabolism: the role of PI3K/AKT/mTOR signalling in pluripotency and cell fate determination. *Development* 2016; 143: 3050–3060.
 37. Nagai S, Kurebayashi Y, Koyasu S. Role of PI3K/Akt and mTOR complexes in Th17 cell differentiation. *Ann N Y Acad Sci* 2013; 1280: 30–34.
 38. Allen MP, Xu M, Linseman DA, Pawlowski JE, Bokoch GM, Heidenreich KA, Wierman ME. Adhesion-related kinase repression of gonadotropin-releasing hormone gene expression requires Rac activation of the extracellular signal-regulated kinase pathway. *J Biol Chem* 2002; 277: 38133–38140.
 39. Allen MP, Linseman DA, Udo H, Xu M, Schaack JB, Varnum B, Kandel ER, Heidenreich KA, Wierman ME. Novel mechanism for gonadotropin-releasing hormone neuronal migration involving Gas6/Ark signaling to p38 mitogen-activated protein kinase. *Mol Cell Biol* 2002; 22: 599–613.
 40. Shankar SL, O'Guin K, Cammer M, McMorris FA, Stitt TN, Basch RS, Varnum B, Shafit-Zagardo B. The growth

- arrest-specific gene product Gas6 promotes the survival of human oligodendrocytes via a phosphatidylinositol 3-kinase-dependent pathway. *J Neurosci* 2003; 23: 4208–4218.
41. Luo H, Cheng J, Han JS, Wan Y. Change of vanilloid receptor 1 expression in dorsal root ganglion and spinal dorsal horn during inflammatory nociception induced by complete Freund's adjuvant in rats. *Neuroreport* 2004; 15: 655–658.
42. Myers SH, Brunton VG, Unciti-Broceta A. AXL inhibitors in cancer: a medicinal chemistry perspective. *J Med Chem* 2016; 59: 3593–3608.